American Mineralogist, Volume 70, pages 549–558, 1985

Heterogeneous distribution of nickel in hydrous silicates from New Caledonia ore deposits

ALAIN MANCEAU AND GEORGES CALAS

Laboratoire de Minéralogie et Cristallographie, LA CNRS 09
Universités de Paris 6 et7
4 place Jussieu 75230 Paris Cedex 05 France
and
Laboratoire pour l'Utilisation du Rayonnement Electromagnétique
(LURE),CNRS,91405 Orsay France

Abstract

Four nickel-bearing clay minerals from New-Caledonia belonging to the lizardite–nepouite and the kerolite–pimelite series have been investigated in order to study the mechanisms of Ni–Mg substitution. Local order around Ni was determined by optical absorption spectroscopy and X-ray absorption spectroscopy at the Ni–K edge. Optical spectra have been reinterpreted through the Kubelka and Munk formalism which lead us to reject the optical evidences for the trigonal distortion of the octahedral Ni site. New data were also obtained concerning Mg–Ni ordering in these minerals. Analysis of the Extended X-ray Absorption Fine Structure (EXAFS) indicates that the intracrystalline distribution of nickel is not random: Ni atoms are segregated into discrete domains, the minimal size of which have been calculated and are interpreted differently depending on whether the mineral belongs to the 7Å (solid state transformed) or to the 10Å (solution precipitated) structure type. This departure from ideal behavior of the Mg–Ni substitution is compared to the chemical and structural variations involving modulated structures. These heterogeneities seem to be quite common in low temperature formation conditions.

Introduction

Nickel concentrations resulting from the weathering of ultrabasic rocks under tropical conditions have been the subject of numerous studies in order to understand better the physico-chemical processes which lead to these ore bodies. Their complex mineralogy is characterized by a mixture of various hydrous silicates, often referred to as "garnierites". The two main minerals (Brindley and Hang, 1973) are lizardite (serpentine) and kerolite (10Å talc), the nickeliferous end-members of which are nepouite (Maksimovic, 1973; Brindley and Wan, 1975) and pimelite (Maksimovic, 1966; Brindley et al., 1979), respectively. Associated phases include smectites and more rarely chlorites and sepiolites. Intimate mixing of 10Å and 7Å phases is clearly exhibited on X-ray diffraction patterns and has been confirmed recently by high-resolution electron microscopy (Uyeda et al., 1973; Pelletier, 1984). It is therefore usually difficult to obtain monomineralic phases by mechanical separation.

Several studies have already been published concerning optical absorption spectra of 1:1 Ni-hydrous silicates (Nussik, 1969; Lakshman and Reddy, 1973; Faye, 1974) but only recently was the crystal chemistry of Ni in these phases precisely studied by these techniques (Cervelle and Maquet, 1982). These authors concluded that Ni^{2+} ions are in 6-fold coordination and occupy sites of C_{3v} symmetry in lizardite. Spectroscopic data concerning nickel in other phyllosilicates are still scarce (Brindley et al., 1979). Furthermore the local order beyond the first coordination shell is not known in any of these phases and limits knowledge of the substitution processes in these Mg–Ni minerals.

In this paper we present first results of a systematic study of nickel-bearing phyllosilicates (Manceau, 1984) by means of various spectroscopic techniques. Diffuse reflectance and K-edge absorption spectroscopies are used to obtain precise crystal chemical parameters concerning the first coordination shell whereas Extended X-ray Absorption Fine Structure (EXAFS) gives data on local order at a scale of several angstroms. The results obtained on carefully selected new-caledonian samples are used in discussing intracrystalline distribution in the two main series, namely lizardite–nepouite and kerolite–pimelite.

Location and characterization of the studied samples

The nickel ore deposits of New Caledonia have been extensively investigated (Trescases, 1975; Troly et al., 1979; Pelletier, 1984). Three horizons may be separated in the alteration zone: (1) the ultrabasic parent rock, mainly of harzburgitic composition; (2) the silicated zone resulting from hydrothermal alteration of this parent rock and consisting of primary lizardite, which was subsequently transformed by supergene processes; (3) the lateritic zone, mostly consisting of Fe-oxyhydroxides. Nickel-bearing clay minerals originate either from transformation of primary lizardites or from solution precipitation (neoformation) in cracks. For this study we have selected a Mg–Fe–Ni lizardite, a pimelite and a Mg–Ni kerolite which were sampled at Poro and Nepoui Mines in

0003–004X/85/0506–0549$02.00

veins inside the silicated zone underlying the lateritic zone. The two latter samples are characteristic of the most abundant Ni-containing neoformed minerals of the garnierites. A nepouite was also collected at Kongouhaou Mine near Thio where it occurs together with weathered chlorite in veins cutting the silicated as well as the lateritic zones.

First, all samples were hand-picked with care under a binocular microscope and homogeneous parts of the garnierites were chosen. Then, only the pure phases were selected by means of powder X-ray diffraction, and characterized by Scanning Electron Microscopy (SEM) and Transmission Electron Microscopy (TEM) associated with electron microdiffraction. Nepouite occurs as well individualized macrocrystallites of 0.2 to 1.0 mm thickness (Fig. 1a). It is made up of regularly superimposed layers which result in the transformation of chlorite. The internal texture of these crystallites was revealed by TEM to be constituted of platy particles which display a mosaic structure (Fig. 1b). Because of the excellent crystallinity the X-ray diffraction patterns exhibit very strong basal reflections. Contrary to the nepouite, the Mg–Fe–Ni serpentine shows tiny particles of about 400Å size with regular rims of a lizardite-like mineral (Fig. 1c). Kerolite and pimelite exhibit a 10Å basal reflection and their behavior with ethylene glycol and heat treatments is characteristic of these minerals (Brindley et al., 1977). After treatment with ethylene glycol for 15 hours, one cannot observe a definite maximum of the 001 peak; in some samples the apparent basal distance expands from 9.36Å to about 16Å whereas in others little expansion occurs (Fig. 2). This difference in expansivity among samples depends on several parameters including layer charge and stacking disorder.

Chemical analyses by atomic absorption spectroscopy are reported in Table 1. The low totals of oxides must be attributed to the high H_2O^+ content occurring in these minerals (Brindley and Wan, 1975; Brindley et al., 1979; Gerard and Herbillon, 1983). In contrast with kerolite and pimelite, lizardite contains varying amounts of iron depending on its origin (Pelletier, 1984). Significant amounts of iron (i.e., more than 1.5%) indicate a primary (hydrothermal) origin followed by supergene transformation whereas iron-poor phases are neoformed (secondary) in garnierites. The structural formulae were calculated assuming a total cation charge of 14 per unit cell for 1:1 phyllosilicates, and of 22 for 2:1 phyllosilicates. Tetrahedral positions are filled with Si atoms together with Al and trivalent Fe to ensure a number of two 4-fold coordinated atoms in TO clay minerals and four atoms in the TOT series. Octahedral sites are filled with (Mg,Ni) atoms and with the remaining Al and Fe^{3+}. The main features of these analyses are that tetrahedral cations exceed two atoms per unit cell in the studied serpentines and are slightly less than four in talc-like samples. These deviations have been repeatedly pointed out by Brindley et al. (1977, 1979) and Gerard and Herbillon (1983). They are consistent with the assumption of lizardite impurities intimately mixed with 2:1 layers in the kerolite–pimelite series and with the presence of silica gels and possibly 2:1 minor phases in the lizardite–nepouite series (Pelletier, 1984; Manceau, 1984).

Spectroscopic characterization of the Ni-site

Nickel crystal chemistry was studied by means of two spectroscopic techniques: diffuse reflectance spectroscopy and Ni *K*-edge structure using synchrotron radiation. Both techniques are related in that they give the same kind of information concerning the first coordination shell, i.e., oxidation state, coordination number, site distortion and metal-ligand covalency. The determination of the actual

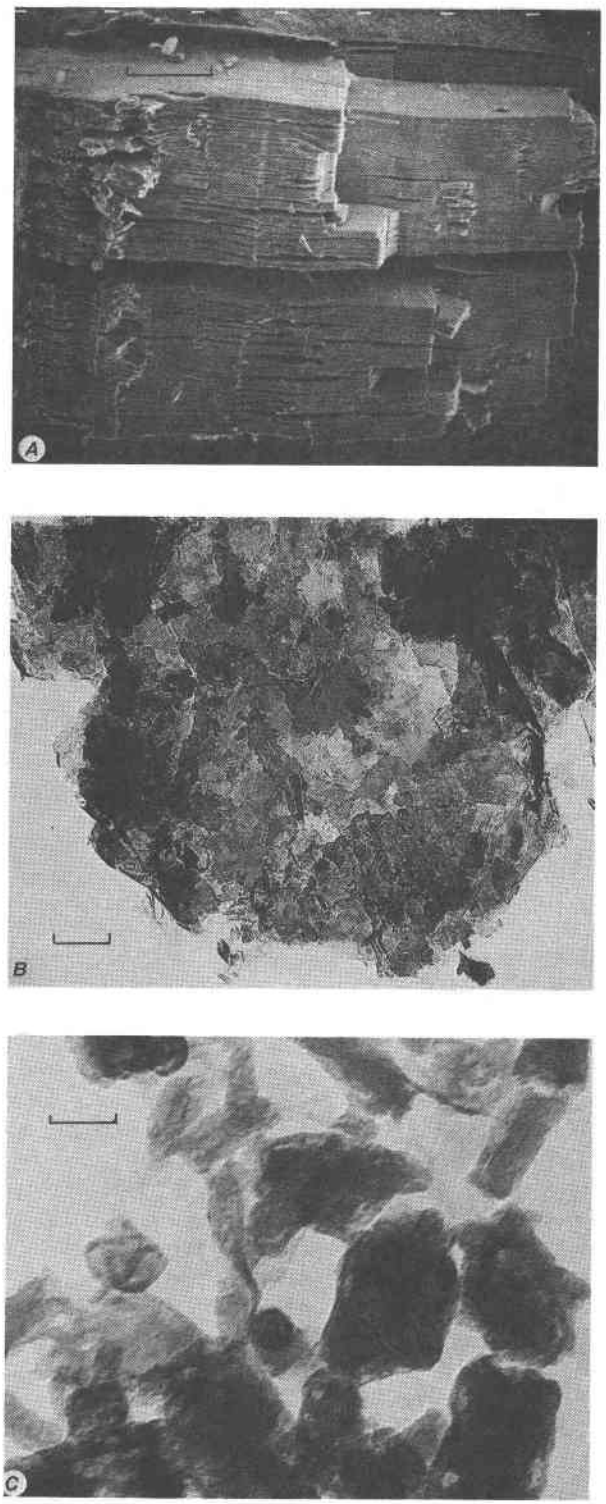

Fig. 1. (a) Scanning electron microscope photographs of a macrocrystallite of nepouite from Thio. Scale marks 50 μm. (b) Transmission electron micrograph showing a detail of the nepouite layers. Scale marks 1 μm. (c) Transmission electron micrograph of a Mg–Fe–Ni lizardite. Scale marks 800Å.

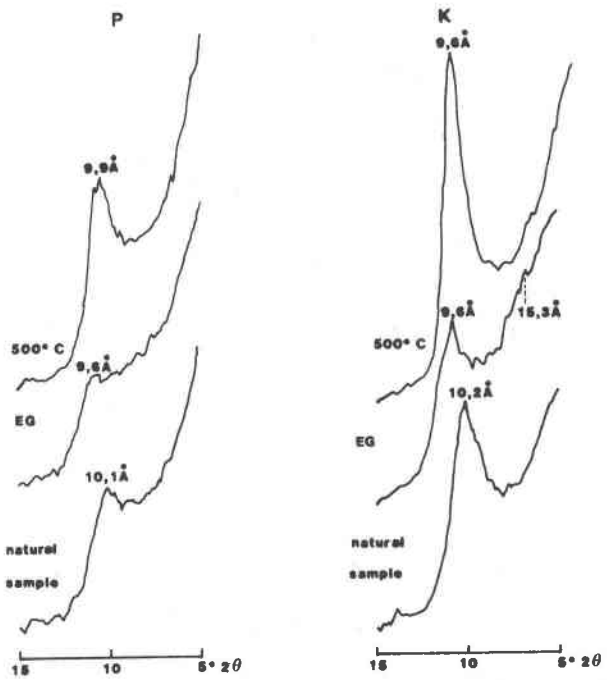

Fig. 2. X-Ray powder diffraction patterns of kerolite and pimelite: behavior with ethylene glycol (EG) and heat treatments. Co$K\alpha$ radiation 1° 2θ/mn.

site symmetry of nickel in lizardite was recently published by Cervelle and Maquet (1982) on the basis of optical absorption spectra. These authors concluded that the octahedral sites occupied by the Ni atoms exhibit a trigonal distortion, with significant differences depending on the nickel concentration in the mineral. This site symmetry agrees with the structure proposed by Pavlovic and Krstanovic (1980) from X-ray diffraction. Our purpose is thus to compare the Ni-behavior in the two main hydrous silicate families of the garnierites.

Table 1. Chemical analysis and structural formulae of Mg–Fe–Ni lizardite (L), nepouite (N), Mg–Ni kerolite (K) and pimelite (P)

	L	N	K	P
SiO_2	42.20	32.60	52.71	45.00
Al_2O_3	0.15	1.43	-	-
Fe_2O_3	2.57	1.57	0.11	0.25
MgO	35.00	4.47	21.10	3.04
NiO	4.50	47.57	14.39	38.94
Total	84.42	87.64	88.31	87.23
Si	2.06	1.99	3.79	3.82
Al	-	0.01	-	-
Fe(III)	-	-	0.01	0.02
Tetr.	2.06	2.00	3.80	3.84
Al	0.01	0.09	-	-
Fe(III)	0.09	0.07	-	-
Mg	2.55	0.41	2.26	0.38
Ni	0.18	2.34	0.83	2.66
Oct. *	2.83	2.99	3.09	3.04

* Oct. = $R^{2+} + 3/2R^{3+}$
L Poro, New Caledonia. N Thio, New Caledonia.
K Nepoui, New Caledonia. P Poro, New Caledonia.

Discussion of the optical absorption spectra

Experimental. Optical spectra were obtained using a Cary 17D spectrophotometer connected to a PDP 11/04 computer. The data were recorded at 1.5 nm intervals by averaging ten measurements for each step. Spectra of nickeliferous minerals were recorded in diffuse reflectance mode, with $BaSO_4$ as a reference, in order to study the powders already characterized by the previous techniques. The obtained reflectance measurements are subsequently transformed into a remission function

$$F(R) = (1 - R)^2/2R$$

which is equivalent to the absorption coefficient deduced from the Beer-Lambert law (Wendlandt and Hecht, 1966). On a wavenumber basis, the spectra may be fitted into gaussian components in order to discuss site energies and possible departure from pure octahedral symmetry (Mendell and Morris, 1982).

Reference for octahedral symmetry: nickel hexahydrate. Optical absorption spectrum of aqueous solution of nickel sulfate is known to be characteristic of a pure octahedral Ni site (Burns, 1970; Cotton and Wilkinson, 1968). We have recorded the spectrum of a 0.5M solution as a basis for our decomposition scheme of the spectra of nickeliferous clay minerals (Fig. 3). The decomposition exhibits three main components at 8510 cm^{-1}, 13868 cm^{-1} and 25460 cm^{-1}, together with spin-forbidden bands of low intensity which occur in the visible range. The position and assignments of the responsible transitions are reported in Table 2. It is to be pointed out that the intense spin-allowed transition at 8510 cm^{-1}, which is directly related to the crystal field splitting, has a pure gaussian shape: this con-

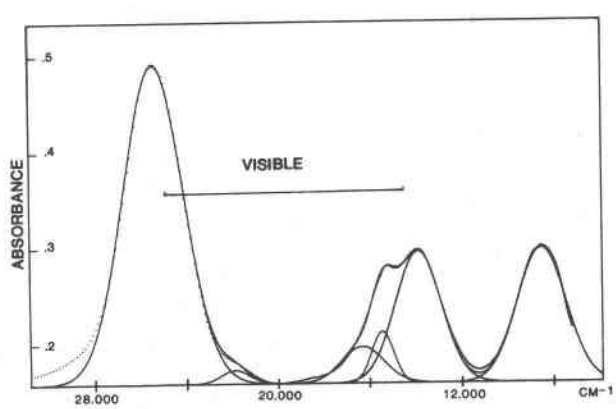

Fig. 3. Optical absorption spectrum of aqueous nickel sulfate. The absorbance is plotted versus wavenumber (cm^{-1}). Dotted line: experimental spectrum. Solid line: gaussian decomposition and sum of the gaussian components.

Table 2. Assignment of absorption bands in the visible and near-infrared obtained by decomposition of the optical spectra with gaussian components

Nature of the transition from the $^3A_{2g}$ level	Aqueous solution of Ni sulfate		kerolite	
	Energy (cm^{-1})	width (cm^{-1})	Energy (cm^{-1})	width (cm^{-1})
$^3T_{2g}(F)$	8510	2484	8950	2435
$^1E_g(D)$	13868	2338	13575	1656
$^3T_{1g}(F)$	15426	1120	15377	2143
	16302	2143	17325	3750
$^1T_{2g}(D)$	21855	1461	22342	2679
$^1A_1(G)$			23900	1558
$^3T_1(P)$	25460	3068	25800	3117

firms the octahedral (O_h) point symmetry of the site. The other transitions at higher energy are rather more complex: spin-orbit coupling may act on the splitting of the $^3T_{1g}$ band, as in crystalline nickel sulfates (Lakshman and Jacob, 1983). We ensured that the optical spectra deduced from reflectance measurements through the remission function F(R) give similar results in the case of non-distorted sites (nickel-doped magnesium and ammonium-magnesium hydrous sulfates, nickel fluosilicate), mainly based on the pure gaussian shape of the absorption band related to the crystal field.

Optical spectra of Ni-hydrous silicates. All the recorded spectra exhibit three absorption bands characteristic of six-fold coordinated divalent nickel (Marfunin, 1979). The corresponding remission functions may be decomposed according to the same scheme as for the undisturbed octahedral site, using gaussian components with about the same width (e.g. the kerolite spectrum: Fig. 4 and Table 2). The disagreement with the previous data (Cervelle and Maquet, 1982) arises from the use of the remission function instead of the raw reflectance data: these latter—although they give correct values of the absorption maxima—do not allow the use of the formalism currently used for interpreting absorbance measurements, such as a fitting procedure into gaussian components. It is interesting to point out that the optical spectra are not sensitive, under the precision of the Kubelka-Munk approximation, to the trigonal distortion of the Mg site in lizardite revealed by the structure refinement (Pavlovic and Krstanovic, 1980; Mellini, 1982).

The crystal field splitting parameter Dq is given by the energy of the $^3A_{2g} \rightarrow {}^3T_{2g}$ transition, which allows to calculate the Crystal-Field Stabilization Energy (CFSE) of nickel in the four studied samples (Table 3). When taking into account the precision of the decomposition procedure the accuracy of the CFSE values is about ± 0.1 kCal/mole. The CFSE decreases in the following order:

nepouite > pimelite = kerolite > lizardite.

The identity of the values obtained in the kerolite-pimelite series demonstrates that the Mg–Ni substitution processes do not affect the nickel crystal chemistry; this information is important in view of the EXAFS evidence of heterogeneous substitution in these minerals. On the other hand, the marked difference in CFSE values between nepouite and Mg–Fe–Ni lizardite is explained by the structural modification which occurs in this series at high Ni-contents. One of the principal characteristics of the serpentine minerals is a "misfit" between the tetrahedral and the octahedral sheet. The *a,b* parameters of the latter being much higher than those of the tetrahedral sheet, this implies a structural modification for juxtaposing these two sheets. In lizardite there exist two non-equivalent Mg sites, which reduces the lateral *ab* dimension of the octahedral sheet (Krstanovic, 1968; Pavlovic and Krstanovic, 1980; Mellini, 1982). The marked difference in the CFSE values between nepouite and Mg–Fe–Ni lizardite may be explained by a structural modification of the octahedral sheet leading to only one cation site and bringing about a decrease of the b parameter (Cervelle and Maquet, 1982). This structural modification is possible because the Ni^{2+} ions are smaller than the Mg^{2+} ions (0.77Å and 0.80Å respectively, Whittaker and Muntus, 1970).

Structure of the Ni K-edge

The use of X-ray absorption spectra for the study of chemically or structurally disordered systems has recently grown with the generalized use of synchrotron radiation. The radiation is utilized as a powerful white-beam X-ray source with various kinds of applications in mineralogy (Calas et al., 1984). Two distinct parts of the spectra contain different kinds of information: the detailed structure of the *K* (or *L*) edge of the studied element and the Extended X-Ray Absorption Fine Structure (EXAFS) which will be treated in the following section. The *K*-edge structure and energy position carry information about oxidation state,

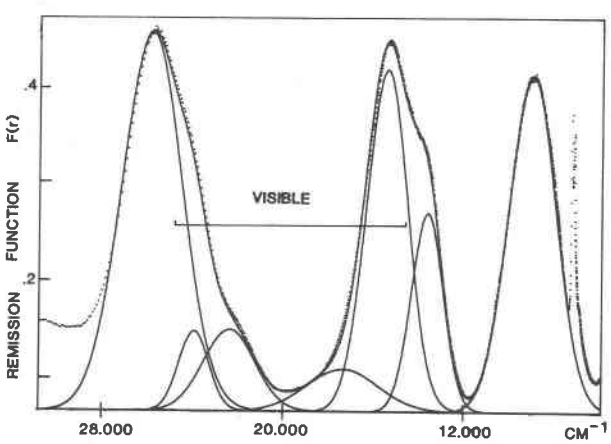

Fig. 4. Optical absorption spectrum of kerolite. The absorbance is plotted versus wavenumber (cm^{-1}). Dotted line: experimental spectrum - Solid line: gaussian decomposition and sum of the gaussian components

Table 3. Crystal chemical parameters of nickel in the investigated minerals

	$^{\S}10\ Dq=\Delta$ (cm^{-1})	$CFSE^{\S\S}$ Kcal/mole	b parameter Å	Ni-O distance	Ni-Ni distance		Number of heavy elements (Ni, Fe) in the second shell		Average dimension of nickeliferous domains
				EXAFS (Å)	X-ray diffraction b/3 (Å)	EXAFS	Structural formulae	EXAFS	
$NiSO_4(H_2O)_6$ solution	8500	29.2	-	-	-	-	-	-	
Reference compound NiO	-	-	-	2.09	-	2.95	12	12	
Reference compound Ni-talc	8950	30.7	9.13	2.08	3.04	3.04	6	6	
Pimelite (P)	8950	30.7	9.14	2.065	3.05	3.05	5.3	5.4±0.5	
Nepouite (N)	9120	31.3	9.17	2.08	3.06	3.06	4.7	6±0.5	
Mg,Ni kerolite (K)	8950	30.7	9.15	2.07	3.05	3.06	1.7	4.7±0.5	15Å-40Å
Mg, Ni, Fe lizardite (L)	8845	30.4	9.20	2.09	3.07	3.06	0.4	4.9±0.5	18Å-60Å

$^{\S}10\ Dq$ = Crystal Field Splitting.

$^{\S\S}CFSE$ = Crystal Field Stabilization Energy.

coordination number, site distortion and metal-ligand covalency. As the theoretical aspects are not precisely known yet, it is necessary to work by comparing the studied samples with well known reference compounds where these various effects may be clearly separated.

The spectra were obtained at the Laboratoire pour l'Utilisation du Rayonnement Synchrotron, Orsay, France (LURE) using the radiation of the DCI storage ring (1.72 GeV). The experimental apparatus has already been described (Raoux et al., 1980). High spectral resolution is obtained with a "channel-cut" monochromator using the 400 reflection of silicon. Intrinsic limitations (core-level width) and experimental conditions permit resolution of features separated by about 1.2 eV. However, because of the excellent stability of the beam, it is possible to detect relative energy shifts as small as 0.2 eV.

Absorption *K*-edges of nickel in the studied clay minerals are shown in Figure 5 together with two reference samples, a 0.5 M aqueous solution of nickel sulfate and $LaNiO_3$ (Ni^{3+}: Crespin et al., 1983). Of the various edge features, only the pre-edge region is well known. It occurs on the low energy side of the edge at about 8326 eV, which is attributed to a transition of 1s electrons to 3d orbitals through a partial hybridization with the 2*p* oxygen orbitals. Its low intensity may be partly explained by the presence of only two holes in the 3*d*-like levels in the divalent nickel ($3d^8$ ion) but the predominant fact is that nickel is in octahedral sites: the tetrahedral symmetry is known to enhance significantly this pre-edge, as was shown in Ni-containing glasses (Petiau and Calas, 1982). The first inflexion point may be used as an indication of the oxidation state of the metal: it shows a 3.8 eV shift towards the higher energies in the Ni^{3+} reference vs. the aqueous solutions of Ni^{2+}. Based on the observed dependence of edge energy on oxidation state and coordination number in Fe silicates and a comparable trend in Ni silicates, the position of this inflexion point suggests that Ni in these hydrous silicates is divalent. The splitting of the maximum

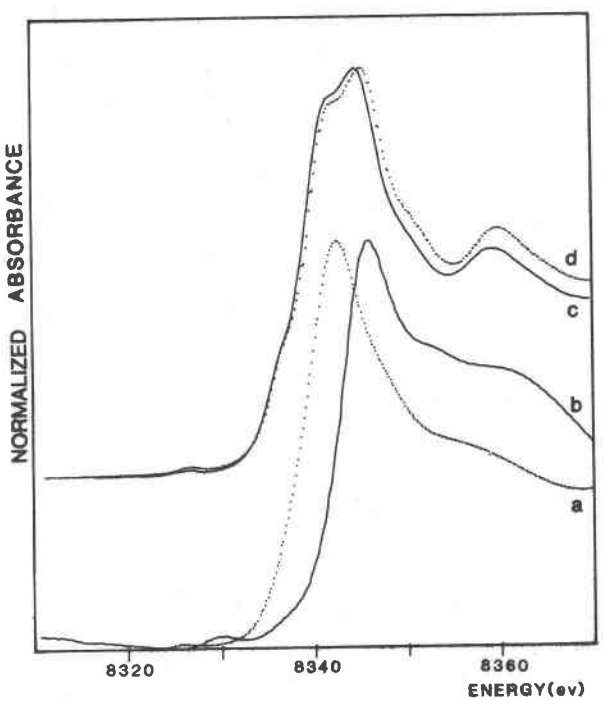

Fig. 5. X-ray absorption *K*-edge structure of Ni in 6-fold coordination: a) aqueous nickel sulfate (0.5 M); b) $LaNiO_3$ (Ni^{3+}) from Crespin et al., 1983; c) nepouite and Mg–Ni–Fe lizardite; d) pimelite and Mg–Ni kerolite.

observed in these latter phases may be interpreted as resulting from a weak site distortion, by comparison with Fe-bearing minerals (Calas and Petiau, 1983; Waychunas et al., 1983). It is to be pointed out that in nickel hexahydrate, where the Ni coordination is a regular octahedron, the *K*-edge does not exhibit such a splitting. The *K*-absorption edge structure of the Ni-bearing minerals are very similar. Therefore, the Ni site geometries are thought not to vary much, in agreement with the conclusions reached from the optical spectra. Moreover, it may be concluded that neither optical nor *K*-edge spectra provide evidence for significant amounts of Ni^{3+}. Trivalent nickel would have given specific additional features on optical spectra. Furthermore, the oxidation state, which can be determined from the "chemical shift," is classically determined by the energy position of the absorption slope as the energy of the crest is also sensitive to the site symmetry. The shape of the Ni *K*-edge of these Ni phyllosilicates is thus fully consistent with divalent nickel. In addition, a recent study of the Ni "pre-edge" peak of these samples under high resolution conditions (Manceau and Calas, to be published) showed no shift of the maximum relative to hexa-aqua Ni^{2+} complexes in solution.

Distribution of nickel in the octahedral sheet

The possibility of a clustered (heterogeneous) arrangement of a certain type of cation in octahedral sheets of phyllosilicates versus a random (homogeneous) arrangement cannot be evaluated by the previously used spectroscopic techniques, which are only sensitive to the first coordination shell. In contrast Extended X-ray Absorption Fine Structure (EXAFS) which extends to several hundred eV above an absorption edge can give information about first, second, and in certain cases, more distant shells. This technique is particularly suitable for structural studies of amorphous and poorly organized compounds and has been applied to various mineralogical systems (see the review of Calas et al., 1984). The information obtained involves interatomic distances between the absorbing atom and the first coordination shells and the number and chemical nature of neighbors in the shell; generally the nearest and next-nearest neighbors may be studied and in simple systems some information may also be derived concerning the third coordination shell.

Acquisition and analysis of EXAFS spectra

The experimental technique is the same as for study of edge structure, although the spectral resolution in EXAFS is not as important as for study of edge structure. For comparison purpose all the spectra were recorded in the same experimental session during dedicated runs at LURE. Figure 6 shows the X-ray absorption spectrum of nepouite near the Ni K-edge. One separates the edge region which was studied in the previous section from the EXAFS which begins from about 60 eV to several hundred eV above the absorption edge. The theory of *K*-EXAFS is now firmly established (Lee et al., 1981) and a quantitative analysis of the experimental spectra is thus made possible.

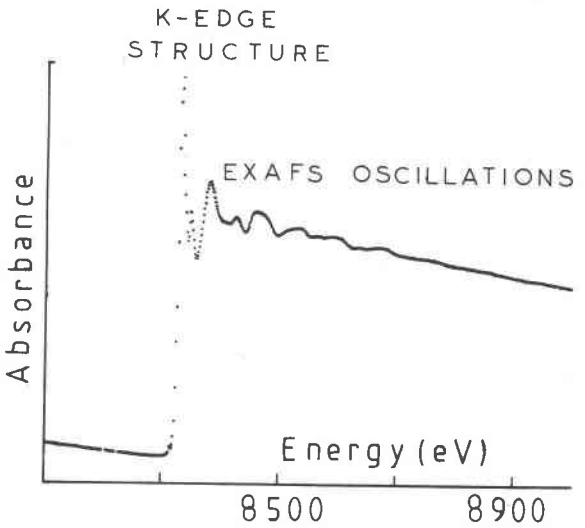

Fig. 6. Whole X-ray absorption spectrum at the Ni *K*-edge of nepouite showing the edge region and the EXAFS oscillations.

The EXAFS is basically an interference phenomenon between the photoelectrons ejected at the absorption edge and those which are backscattered by the various surrounding atomic shells. It may be described by a sum of damped sinusoids which depend on the photoelectron wavevector k according to the relationship

$$\chi(k) = \frac{1}{k} \sum_j A_j(k) \sin (2kR_j(k) + \psi_j(k))$$

where the index j refers to the scattering by the jth atomic shell. R_j is the distance between the absorber atom and the jth shell, ψ_j is a phase factor due to both the central and the backscattering atoms, and $A_j(k)$ is the amplitude factor

$$A_j(k) = \frac{N_j}{R_j^2} f_j(k, \pi) e^{-2}\sigma_j^2 k^2 e^{-2R_j/\lambda}$$

where N_j is the coordination number on the jth shell, $f_j(k, \pi)$ the backscattering amplitude function corresponding to the atomic species on this shell, σ_j is the standard deviation of the R_j distances and λ the mean free path length of the photoelectron.

To ensure the reliability of the comparison between the studied samples we have used the same parameters in the analysis procedure for all of them. First the X-ray absorption background A(O) is removed from the experimental spectrum by substracting a Victoreen function in a region beginning about 300 eV below the absorption edge. The mean absorption A(1) of the sample above the edge is obtained by fitting a polynomial function. The EXAFS oscillations $\chi(E)$ (Fig. 7) are obtained from

$$\chi(E) = (A(E) - A(1))/(A(1) - A(O)),$$

where A(E) is the experimental absorbance. The energy scale (E) is subsequently converted into a wavevector scale (k), by choosing the reference energy E_o at the inflexion

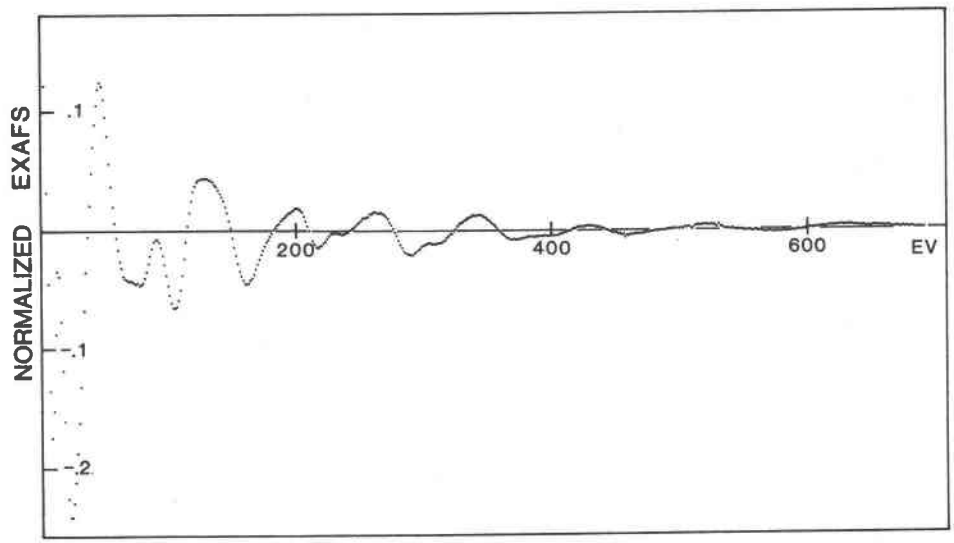

Fig. 7. Normalized EXAFS of the nepouite. Normalized $\ln(I_0/I)$ is plotted versus photon energy (eV).

point of the Ni *K*-edge (E_0 = 8340 eV). A Fourier transform is performed on the function $k.\chi(k)$. As the shape of the windows used for computing this Fourier transform may strongly influence it, we used constant transformation conditions, a flat window in the range 3.7Å^{-1}–11.2Å^{-1} ended on both sides by a cosine function of 0.5Å^{-1} width.

The magnitude of this Fourier transform concerning the four minerals studied in the previous section is reported in Figure 8, together with the Ni-talc (willemseite) as a reference compound whose Mg analog has a well known structure (Rayner and Brown, 1973). It is possible to get the contribution of a definite shell to the EXAFS by backtransforming the corresponding peak on the Fourier transform into the k-space. Figure 9a shows the damped sinusoid obtained by backtransforming the second peak of the willemseite. The interatomic distances are calculated by using theoretical phase shifts $\psi(k)$ (Teo and Lee, 1980). The validity of these phase shifts was confirmed by studying crystalline references, namely willemseite and bunsenite (NiO). On account of the agreement of the EXAFS data with the actual Ni–O and Ni–Ni distances in these compounds, the accuracy of the distance measurements is estimated to be 0.02Å; a relative precision of about 0.01Å may be attained by comparing spectra studied under identical treatment conditions.

The first peak of the Fourier transform (Fig. 8) is assigned to the oxygen coordination shell: the corresponding Ni–O distances are reported in Table 3. They confirm the octahedral site of nickel in all the studied compounds. The second peak corresponds to the next nearest neighbors, Ni, Fe or Mg. It is assigned to the Ni–Ni distance in NiO and Ni-talc, but we must discuss in more detail the chemical nature of the atoms constituting this shell for the minerals which have a more complex composition.

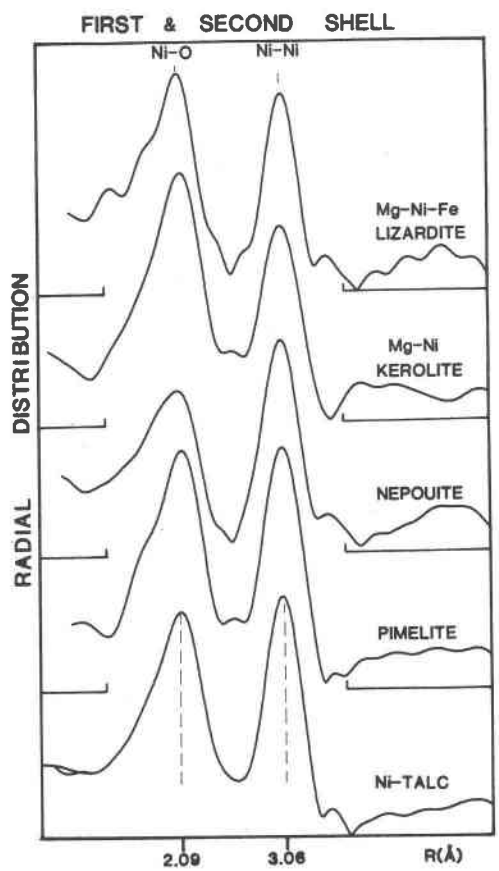

Fig. 8. Comparison of the partial distribution function (Fourier transform modulus curve) of the EXAFS spectra at the Ni *K*-edge of five Ni-bearing clay minerals.

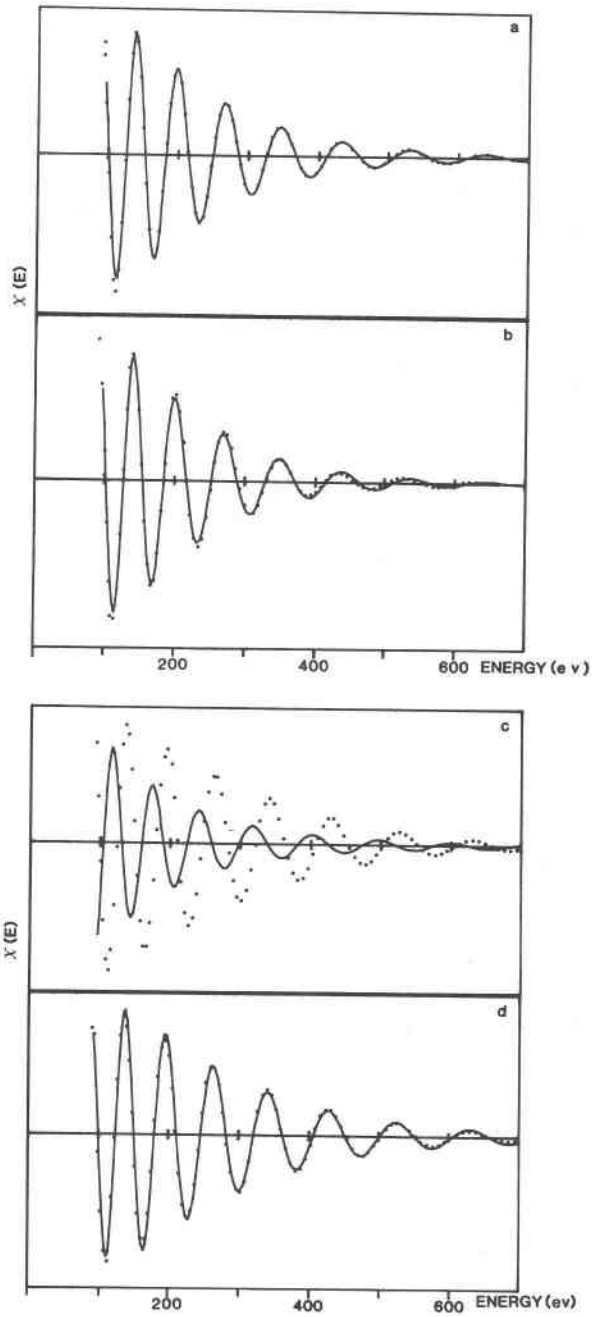

Fig. 9. Fourier filtered contribution of the second shell (dotted line) and the corresponding calculated curve (solid line) based on theoretical phase shift and backscattered amplitude values of Teo and Lee (1980): a) nepouite: 6 Ni neighbors at 3.06Å; b) Ni-talc: Ni atoms are surrounded by 6 Ni neighbors at 3.04Å; c) the same sample as d), but calculations are performed by assuming 6 Mg neighbors at 3.07Å: the fit is clearly unacceptable; d) Mg–Fe–Ni lizardite: 4.4 Ni neighbors at 3.06Å.

Evidence for heterogeneous distribution of nickel

The nickel end members of the two series under investigation are characterized by a second shell constituted only by Ni atoms. As $b/3$ is equal to the metal–metal distance, the Ni–Ni distances which are calculated by EXAFS analysis are compared to the $b/3$ values obtained by X-ray diffraction from the 06.33 reflection in Table 3. The good agreement between both techniques confirms the validity of our analysis.

The study of minerals of low Ni-content is more difficult to perform because some assumptions must be made concerning the constitution of the second shell around Ni as the phase shifts $\psi(k)$ depend on the chemical nature of the backscattering atom. We performed two calculations, first by assuming that all the atoms of the second shell are transition elements (Ni and Fe have similar backscattering phases and amplitudes and cannot be distinguished by EXAFS), then by assuming only Mg atoms in this shell. The structural constraint is given by X-ray diffraction of these minerals which shows that the b parameter and thus the cation–cation distances are close in the kerolite–pimelite and in the nepouite–lizardite series (Table 3). This may be explained by the similar ionic radii of Mg and Ni (0.80Å and 0.77Å, respectively).

The fact that the interatomic distance is well defined allows us to overcome the indetermination about the nature of the second nearest neighbors. This is true because the distance determined by EXAFS varies depending on the type of backscattering atom, and inversely it is possible to determine its type by knowledge of the actual distance. Distance determination is made by considering the contribution of one shell to the whole EXAFS spectrum by back-transforming the corresponding peak in the real space into the k space (Fig. 9b) and calculating the zeros of this function. If we use the EXAFS formula as defined above, a theoretical curve may be calculated by adjusting three parameters: the number and nature of the surrounding atoms (this latter affects both phase shift and amplitude values) and the corresponding inter-atomic distances. Only the latter two are used for distance calculation as they determine the zeros of the sine function. The Debye-Waller parameter was fixed to 0.09Å, the value determined for the reference compound. A good agreement is found between the experimental and calculated curves (Fig. 9b and 9d) by taking nickel (or iron) as the backscattering atom and the Ni–(Ni,Fe) distances determined from XRD (3.05–3.06Å). On the contrary, it is not possible to get a correct fit by considering a second shell only composed by Mg atoms (Fig. 9c) unless the Ni–Mg distance is set at the unrealistic value of 3.13Å. Since nickel is essentially surrounded by heavy atoms even in clay minerals of low (Fe,Ni) content, we have evidence for the heterogeneous character of the substitution of Mg by transition elements.

Estimation of the size of the Ni-enriched areas

As the nature of the atoms present on one coordination shell is known, it is possible to get their number from the amplitude of the corresponding EXAFS. The backscattering amplitude of nickel was calculated from the theoretical values of Teo and Lee (1980) and found to be valid by

analysis of the willemseite as a reference compound for the clay minerals we investigated. The number of Ni second neighbors found by EXAFS in Ni end-members nepouite and pimelite is in good agreement with the structural formulae (Table 3). In the phases of low-(Ni,Fe) content it must be noticed that the second peak has a similar intensity as for the reference compounds, which indicates the presence of predominant (Ni,Fe) atoms on the second shell. It must be noticed that the difference between the backscatterer phase of Mg and Ni is about π; therefore the presence of some Mg atoms together with Ni atoms on the second coordination shell would tend to decrease the amplitude of the wave backscattered by the surrounding atoms. EXAFS cannot separate the contributions of heavy atoms from the light ones, as the A(k) function varies almost linearly in both cases in this energy range. Apparent values are $4.4 \pm 0.5$and 4.2 ± 0.5 Ni(Fe) atoms for lizardite and kerolite respectively. If we take into account the phase opposition which exists between Ni and the Mg atoms which complete to six neighbors this second shell we obtain the respective values of 4.9 ± 0.5 and 4.7 ± 0.5. These values must be compared to those estimated from the structural formulae, 0.38 in lizardite and 1.66 in kerolite. We have thus additional evidence for the non-random distribution of nickel in the octahedral layer of these minerals.

The comparison between the number of Ni(Fe) neighbors calculated from structural formulae and measured by EXAFS may be interpreted quantitatively to estimate the average size of the areas which are Ni(+Fe)-enriched. If we assume that these latter have a circular shape and are devoid of Mg atoms, only the atoms at the boundaries of these regions have Mg as neighbors. In this hypothesis we get average diameters of between 20Å (i.e., 2 cell units) and 60Å in Mg–Fe–Ni lizardite and between 15Å and 40Å in Mg–Ni kerolite. In a model assuming a circular shape of these segregated areas, it must be noticed that the mean number of Ni atoms surrounding a central atom increases faster for the small dimensions than for the larger ones. Consequently these calculations are not accurate for the large dimensions. If Mg atoms are present inside these enriched areas, the dimensions obtained are significantly increased. Therefore the average values given above correspond to an lower limit; the upper limit cannot be estimated but may lead to a whole layer. Furthermore, as we have only access to spatially averaged values, a distribution of these dimensions cannot be excluded.

Discussion

The data presented in this study permit discussion of the nickel distribution within the two most abundant Ni-containing series of the garnierites.

Ni–Mg cation ordering in the kerolite–pimelite series

Two types of structural configurations may be considered: (1) Ni and Mg can be clustered within the octahedral sheet or (2) different types of Ni-(Fe) sheets can be irregularly distributed in the phyllosilicate structure. In this latter model the 2:1 phyllosilicates of the garnierites would essentially consist of mixtures of kerolite and pimelite at a scale of several layers. This hypothesis cannot be excluded as it would not be detected by XRD, whereas the optical spectra of both phases are identical.

Ni–Mg cation ordering in the lizardite–nepouite series

The two-cation ordering schemes described previously cannot apply to this series, as the coexistence of Ni- and Mg-layers in the lizardite would give optical spectra similar to that of nepouite. The marked difference between both spectra leads to rejection of this hypothesis. Data available point to the existence of Ni-rich areas of small dimensions without any structural reorganization as it is observed in the nepouite. This discussion refers to the crystallinity of these minerals. From the TEM studies and the presence of a strong 06.33 reflection, we deduce that there is a good crystallinity of the samples in the *ab* planes, with a 200–300Å length of coherence. The Ni-containing areas are smaller than that value.

Conclusion

Few data exist on the actual mechanisms of atomic substitution in minerals. In the case of ions with the same valence, the condition of equality of charges and of ionic radii is not sufficient to imply the existence of ideal solid solutions in minerals. The chemical heterogeneity at a scale of several angstroms that we report in Ni-clay minerals may be compared to the chemical variations bringing about modulated structures shown under high resolution conditions in some minerals and alloys (Buseck and Cowley, 1983). However as EXAFS is not based on any assumption concerning the periodic character of the chemical heterogeneities, we have no information about that parameter and it is unlikely that they could be imaged by HRTEM. The structural problem is the correlation between both scales of observation of these heterogeneities, the middle range order between 5 and 15Å being until now impossible to attain directly either with techniques such as EXAFS (because of the limited mean free path of the photoelectrons) or with imaging techniques. However, the existence of chemical heterogeneity could be related to the growth conditions, with the possible influence of disequilibrium conditions. The distinct behavior of 10Å and 7Å minerals pointed out in this study refers also to distinct geological formation conditions. The lizardite is derived from the transformation of primary serpentines by a Ni-enrichment and a subsequent Mg loss. In contrast, the minerals of the kerolite–pimelite series are solution precipitated products and the existence of distinct Mg- and Ni-octahedral layers can be correlated to this distinct formation process. The comparison of Ni-crystal chemistry among minerals formed under various weathering conditions could lead to a better comprehension of heterogeneous substitution mechanisms, which certainly play an important role in the processes of supergene enrichment of nickel. In summary, the most important result of this study is the discovery of a heterogeneous distribution of Ni (i.e., a clustering) in the octahedral sheet of hydrous Ni layer silicates.

Acknowledgments

The authors wish to thank M. Gilbert Troly and MM. Esterle, Bernard Pelletier and Bernard Escande (Société Métallurgique Le Nickel, SLN) who helped us in the knowledge of the New Caledonian ore deposits and provided facilities during the sampling. We are also grateful to L.U.R.E. for the Synchrotron Radiation facilities, Mrs. Madeleine Gandais and M. Claude Guillemin for TEM studies and Mrs. Hélène Vachey for the chemical analyses. We thank Mrs. Jacqueline Petiau and MM. Gerard Bocquier, G. E. Brown, Bernard Cervelle and Michel Semet for their kind advices. This work is supported by MST/MRI grant, Valorisation des Ressources du Sous-Sol, Contract N°82D-0811.

References

Brindley, G. W., Bish, D. L., and Wan, H. M. (1977) The nature of kerolite, its relation to talc and stevensite. Mineralogical Magazine, 41, 443–452.

Brindley, G. W., Bish, D. L., and Wan, H. M. (1979) Compositions, structures and properties of nickel-containing minerals in the kerolite–pimelite series. American Mineralogist, 64, 615–625.

Brindley, G. W. and Hang, P. T. (1973) The nature of garnierites-I: Structures, chemical compositions and color characteristics. Clays and Clay Minerals, 22, 27–40.

Brindley, G. W. and Wan, H. M. (1975) Compositions, structures and thermal behaviour of nickel-containing minerals in the lizardite–nepouite series. American Mineralogist, 60, 863–871.

Burns, R. G. (1970) Mineralogical Applications of Crystal Field Theory. Cambridge University Press, Cambridge, England.

Buseck, Peter and Cowley, J. M. (1983) Modulated and intergrowth structures in minerals and electron microscope methods for their study. American Mineralogist, 68, 18–40.

Calas, Georges, Bassett, W. A., Petiau, Jacqueline, Steinberg, Michel, Tchoubar, Denise, and Zarka, Albert (1984) Mineralogical applications of synchrotron radiation. Physics and Chemistry of Minerals, 11, 17–36.

Calas, Georges and Petiau, Jacqueline (1983) Structure of oxide glasses: spectroscopic studies of local order and crystallochemistry. Geochemical implications. Bulletin de Minéralogie, 33–55.

Cervelle, B. D. and Maquet, Michel (1982) Cristallochimie des lizardites substituées Mg–Fe–Ni par spectrométrie visible et infra-rouge proche. Clay Minerals, 17, 377–392.

Cotton, F. A. and Wilkinson, G. (1968) Advanced Inorganic Chemistry. Interscience Publishers, New York.

Crespin, Michel, Levitz, Pierre, and Gatineau, Lucien (1983) Reduced forms of $LaNiO_3$ perovskite. Journal of the Chemical Society, Faraday Transactions 2, 79, 1181–1194.

Faye, G. H. (1974) Optical absorption spectrum of Ni^{2+} in garnierite: a discussion. Canadian Mineralogist, 12, 389–393.

Gerard, P. and Herbillon, Adrien (1983) Infrared studies of Ni-bearing clay minerals of the kerolite–pimelite series. Clays and Clay Minerals, 31, 143–151.

Krstanovic, P. (1968) Crystal structure of single layer lizardite. Zeitschrift für Kristallographie, 126, 163–169.

Lakshman, S. U. and Reddy, B. J. (1973) Optical absorption spectrum of Ni^{2+} in garnierite. Proceedings of the Indian Academy of Sciences, A, 77, 269–278.

Lakshman, S. U. and Jacob, S. A. (1983) Absorption spectra of Ni^{2+} in $(NH_4)_2Mg(SO_4)_2 \cdot 4H_2O$. Solid State Communications, 48, 563–568.

Lee, P. A., Citrin, P. H., Eisenberger, P. and Kincaid, B. M. (1981) Extended X-ray Fine Structure: its strength and limitations as a structural tool. Review of Modern Physics, 53, 769–806.

Maksimovic, Z. (1966) Kerolite–pimelite series from Goles mountain, Yugoslavia. Proceedings of the International Clay Conference, Jerusalem, 1, 97–105.

Maksimovic, Z. (1973) Lizardite–nepouite isomorphic series. Zapiski Mineralski Obslich, 102, 143–149.

Manceau, Alain (1984) Localisation du nickel dans les phyllosilicates: conséquences sur les conditions de formation des minerais de nickel de Nouvelle-Calédonie. Thèse de Spécialité, Université de Paris VII.

Marfunin, A. S. (1979) Physics of Minerals and Inorganic Materials. Springer Verlag, Heidelberg.

Mellini, M. (1982) The crystal structure of lizardite 1T: hydrogen bonds and polytypism. American Mineralogist, 67, 587–598.

Mendell, W. W. and Morris, R. V. (1982) Band quantification in reflectance spectroscopy. Lunar and Planetary Science XIII, 513–514.

Nussik, S. A. M. (1969) Optical absorption spectra of Ni-bearing minerals. Izvestia Akademia Nauk SSSR, Geol. Series, 3, 108–112.

Pavlovic, S. and Krstanovic, P. (1980) Order-disorder structure in lizardite. Bulletin de l'Académie Serbe des Sciences et Arts, 20, 55–58.

Pelletier, Bernard (1984) Localisation du nickel dans les minerais "garniéritiques" de Nouvelle-Calédonie. In D. Nahon, Ed., International Congress on Alteration Petrology, CNRS, Paris. Sciences Géologiques 73, 173–183.

Petiau, Jacqueline and Calas, Georges (1982) Local structure about some transition elements in oxide glasses using X-ray absorption spectroscopy. Journal de Physique, C9, 47–50.

Raoux, Denis, Petiau, Jacqueline, Bondot, Paul, Calas, Georges, Fontaine, Alain, Lagarde, Pierre, Levitz, Pierre, Loupias, Geneviève, and Sadoc, Anne (1980) L'EXAFS appliqué aux déterminations structurales de milieux désordonnés. Revue de Physique Appliquée, 15, 1079–1094.

Rayner, J. H. and Brown, G. (1973) The crystal structure of talc. Clays and Clay Minerals, 21, 103–114.

Teo, B. K. and Lee, P. A. (1980) Ab initio calculation of amplitude and phase function for Extended X-Ray Absorption Fine Structure (EXAFS) Spectroscopy. Journal of the American Chemical Society, 101, 2815–2830.

Trescases, Jean Jacques (1975) L'évolution géologique supergène des riches ultrabasiques en zone tropicale. Formation des gisements nickélifères de Nouvelle-Calédonie. Mémoires ORSTOM, Série Géologie, 78.

Troly, Gilbert, Esterle, M., Pelletier, Bernard, and Reibel, W. (1979) Nickel deposits in New-Caledonia: some factors influencing their formation. International Laterite Symposium, New-Orleans, 85–119.

Uyeda, N., Hang, P. T., and Brindley, G. W. (1973) The nature of garnierites II. Electron-optical study. Clays Minerals Bulletin, 21, 41–50.

Waychunas, G. A., Apted, M. J., and Brown, G. E. (1983) X-ray K-edge absorption spectra of Fe minerals and model compounds. Near-edge structure. Physics and Chemistry of Minerals, 10, 1–9.

Wendlandt, W. M. and Hecht, Harry (1966) Reflectance spectroscopy. Interscience Publishers, 298 p.

Whittaker, E. J. W., and Muntus, R. (1970) Ionic radii for use in geochemistry. Geochimica et Cosmochimica Acta, 34, 945–956.

Manuscript received, April 26, 1984;
accepted for publication, December 3, 1984.